Review

GREENHOUSE GASES SCIENCE AND TECHNOLOGY

A review on the solid–liquid–vapor phase equilibria of acid gases in methane

Hani Ababneh and **Shaheen A. Al-Muhtaseb**, Department of Chemical Engineering, Qatar University, Doha, P.O. Box 2713, Qatar

Abstract: In spite of the increasing levels of greenhouse gases in the atmosphere, and their impact on the environment, the demand for natural/biogas will increase significantly in the coming few decades. To cover this demand, the global energy industry is continuously exploiting sour gas reserves located around the world. Nonetheless, sour gas has to be sweetened before the practical utilization of natural or biogas. The cryogenic separation technologies have emerged as a new technology to separate carbon dioxide (CO_2) and hydrogen sulfide (H_2S gases) from natural/biogas. The cryogenic separation produces less harmful gases, and can be less expensive to operate and maintain in comparison to the conventional technologies. To design cryogenic separation equipment, vapor–liquid equilibrium (VLE), solid–liquid equilibrium (SLE), solid–vapor equilibrium (SVE), and solid–liquid–vapor equilibrium (SLVE) data for the corresponding binary systems (of CH_4-CO_2, CH_4-H_2S, and H_2S-CO_2) and ternary system (of CH_4-H_2S-CO_2) are required. The main target of this article is to review the SLVE data for the acid gases (CO_2 and H_2S) in methane (CH_4) as the main constituent of natural/biogas. It will address SLVE data for the binary systems of CH_4-CO_2, CH_4-H_2S and H_2S-CO_2 as well as the ternary system of CH_4-H_2S-CO_2. It will not only address the available laboratory data, but it will also discuss, compare and evaluate the different models used to correlate/predict these data. © 2022 Society of Chemical Industry and John Wiley & Sons, Ltd.

Keywords: natural gas sweetening; solid phase formation; binary/ternary mixture separation; solid–liquid–vapor equilibrium; freezing prediction; cryogenic separation

Introduction

Natural gas is the cleanest traditional energy source. Thus, its demand is expected to increase by 33% in the next 30 years.[1] The increased demand for natural gas and the strictest targets for the share of renewable fuels in the global energy consumption led to an increasing interest in the use of biogas as an alternative source of energy.[2] Natural gas and biogas consist mainly of methane (CH_4), carbon dioxide (CO_2), hydrogen sulfide (H_2S), along with possible traces of water and other pollutants like ammonia, and particulates.[3] Therefore, they have to be refined and upgraded, which is accomplished by separating the sour gases (CO_2 and H_2S) from the methane. Sour gases decreases the specific enthalpy of

Correspondence to: Shaheen A. Al-Muhtaseb, Department of Chemical Engineering, College of Engineering, Qatar University, 2713, Doha, Qatar.
E-mail: s.almuhtaseb@qu.edu.qa
Received January 27, 2022; revised April 17, 2022; accepted May 31, 2022
Published online at Wiley Online Library (wileyonlinelibrary.com). DOI: 10.1002/ghg.2161

the natural/biogas, and are highly corrosive to the pipelines and equipment of natural gas processing plants.[4]

Carbon dioxide (CO_2) has reached an alarming concentration level in the atmosphere. Carbon dioxide resulting from the combustion of fossil fuels accounts for the largest share of global anthropogenic GHG emissions.[5] This has increased the global mean surface-temperature by ∼1°C from the preindustrial era levels.[6] In order to decelerate or stop the global warming phenomena, the demand for cleaner energy sources has increased. Hydrogen sulfide (H_2S) is a colorless component commonly found in natural gas. it is highly corrosive and it caused many failures of pipelines and pressure vessel in the oil and gas industry.[7] In addition to that, H_2S is a very poisonous and flammable gas with an odor similar to that of rotten eggs.[8] The H_2S removed from sour gas can be a precursor for the production of elemental sulfur, and organosulfur compounds such as methanethiol, ethanethiol, and thioglycolic acid.[9]

The most commonly used method in the industry for sweetening natural gas (i.e., removing acid gases) is the solvent (e.g., amine)-based absorption technology. However, this technology suffers from high energy requirements and costly maintenance and operation.[10] Therefore, new technologies have emerged for natural/biogas sweetening, among them is the cryogenic separation. Cryogenic separation is a physical process where acid gases are separated from methane at very low temperatures by benefiting from the differences in their volatility.[11] Advantages of cryogenic separation include its low environmental footprint, applicability in high and low pressure systems, and not requiring additional solvents.[12] Examples of cryogenic separation technologies include conventional cryogenic distillation, extractive cryogenic distillation, cryogenic packed bed separation, and the dual pressure distillation unit.[11] While solid formation within these units is generally avoidable, some separation technologies (such as Controlled Freezing Zone (CFZ)^{TM} process, which is developed by ExxonMobil) benefit from the solid formation to improve the separations process and minimize the cost.[13]

Cryogenic separation techniques involve conventional methods (e.g., liquid–vapor separation), nonconventional methods (e.g., solid–vapor separation),[14] and hybrid methods.[11] The most widely used conventional method is the cryogenic distillation, which operates at very low temperatures and high pressures in order to separate CO_2 from other components based on the differences in their boiling temperatures, where the carbon dioxide is removed either in a high-pressure gas phase or in a liquid phase. Despite the effectiveness of conventional cryogenic methods in separating concentrated CO_2 stream, it is considered an expensive-to-operate technology due to the high energy required to reach high pressures, and the necessity of avoiding solids formation.[14] Nonconventional methods benefit from desublimation or solidification to improve the separation process and reduce the energy requirements.[15] Nonconventional methods usually operate at lower temperatures compared to cryogenic distillation, at which CO_2 will solidify. Even though these sources discuss only the solidification of CO_2, H_2S removal by solidification is similar. Nonconventional technologies include; cryogenic packed beds,[16] moving packed beds,[17] Stirling coolers,[18] cryogenic carbon capture with an external cooling loop (CCC-ECL),[19] and compressed flue gas cryogenic carbon capture with compressed flue gas (CCC-CFG).[19] Hybrid methods combine conventional and nonconventional methods into a single-unit operating system to overcome the disadvantages of conventional methods and produce better or similar results at lower cost than nonconventional technologies.[11] Examples on hybrid methods include the Controlled Freezing Zone (CFZ) technology,[20] Cryocell-based separation[21] and condensed contaminant centrifugal separation.[19]

To design cryogenic separation equipment, vapor–liquid equilibrium (VLE), solid–liquid equilibrium (SLE), solid–vapor equilibrium (SVE), and solid–liquid–vapor equilibrium (SLVE) data for the corresponding binary systems (of CH_4-CO_2, CH_4-H_2S and H_2S-CO_2) and the ternary system (of CH_4-H_2S-CO_2) are needed. Maqsood *et al.*[11] have covered the different cryogenic separation technologies used for separating the binary system of CH_4-CO_2, and they discussed the limitations and operational conditions for each of these processes. However, their review has not focused on the thermodynamic (i.e., phase equilibrium) side of such technologies. Similarly, Tan *et al.*[22] have reviewed the cryogenic separation techniques used for biogas upgrading, while mentioning thermodynamic models used to represent the binary system CH_4-CO_2 but no details or comparison between these models were represented. Babar *et al.*[23] have extensively reviewed the

thermodynamic data for the cryogenic separation of CH_4-CO_2. They reviewed, among the other topics, the experimental phase equilibrium data for CH_4-CO_2 mixture and the predicted data obtained by the different models available in the literature or the computer simulators utilizing some of these models. The VLE, SLE, SVE, and SLVE data were all covered and discussed. However, some experimental data for the SLVE system were not mentioned in that work. Moreover, few thermodynamic models were not covered and no comparison between them was offered.

As per our knowledge, no review papers in the published literature addressed the H_2S solid phase equilibria within different systems; including CH_4-H_2S and H_2S-CO_2 and CH_4-H_2S-CO_2.

The objective of this article is to review the solid–liquid–vapor equilibrium (SLVE) for the acid gases in natural/bio gas; which involves the binary systems of CH_4-CO_2, CH_4-H_2S and H_2S-CO_2 as well as the ternary system of CH_4-H_2S-CO_2. It will include the published experimental data, which include the SLVE locus curve and the composition of each phase at that point. Moreover, this review discusses, compares and evaluates the different models used to predict these data.

Experimental data

Experimental data available for the SLVE locus involving CH_4, CO_2, and H_2S are limited in the literature. This section will give an overview of the experimental data for the binary systems of CH_4-CO_2, CH_4-H_2S, and H_2S-CO_2 as well as the ternary system of CH_4-H_2S-CO_2.

The experimental SLVE data of the binary system CH_4-CO_2 come mainly from four different studies by Donnelly and Katz,[24] Pikaar,[25] Sterner[26] and Davis *et al.*[27] Donnelly and Katz[24] determined the SLVE locus by varying the CO_2 content within the CH_4-CO_2mixtures and finding the phase envelope using a glass windowed pressure cell. They prepared six mixtures with CO_2 concentrations from 0% (pure CH_4) to 88% and tested them at temperatures up to 215.3 K. Pikaar[25] investigated the SLVE locus in a temperature range from 143.15 to 203.15 K, with CO_2 concentrations between 1% and 20%. He noticed a variation between his results and those of Donnelly and Katz at low temperatures, and concluded that the results of Donnelly and Katz maybe inaccurate at temperatures lower than 206.15 K. Sterner measured

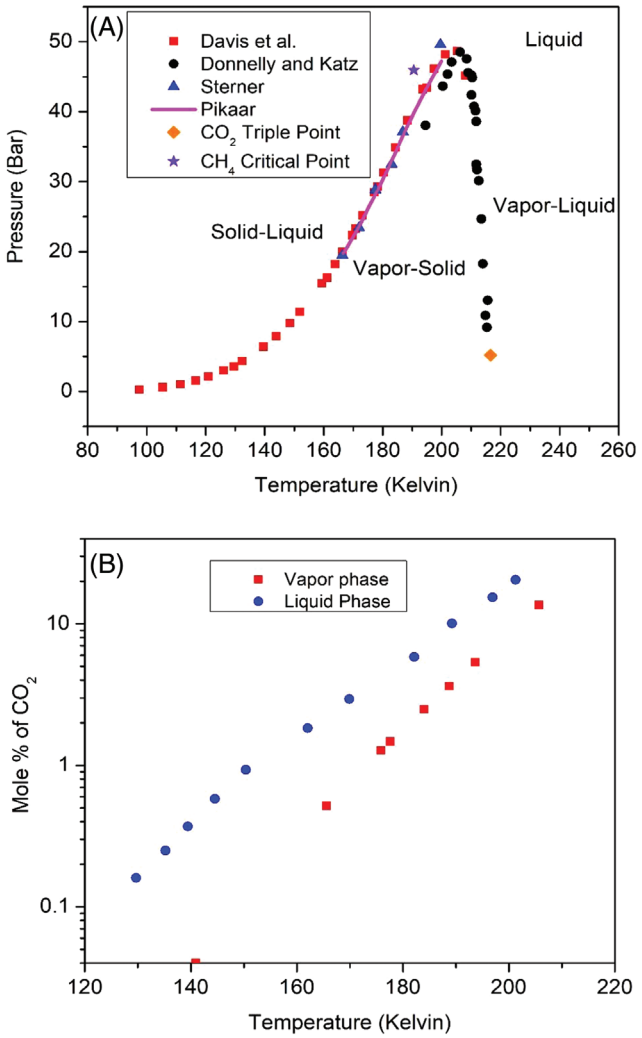

Figure 1. Experimental data available for the binary system CH_4-CO_2 in terms of (A) SLVE locus,[24,25,26,27] CO_2 triple point,[28] CH_4 critical point[29] and (B) corresponding CO_2 compositions in the liquid and vapor phases (while solid phase is pure CO_2).[27]

the SLVE locus at temperatures lower than the critical temperature of pure CH_4.[26] Davis *et al.*[27] measured the SLVE locus starting from the triple point of CO_2 up to a temperature of 97.54 K. Their measurements covered a wide range of temperatures and included the vapor and liquid phase compositions over the locus line. Figure 1(A) compares the results for the four sets of experimental data. On the other hand, only Davis *et al.*[27] reported the compositions of different phases at the SLVE locus of the binary system CH_4-CO_2. They confirmed that the solid phase consists of pure CO_2, while the other two phases (vapor and liquid) contain both components. The liquid and vapor phase

Greenhouse. Gas. Sci. Technol. **12**:566–579 (2022); DOI: 10.1002/ghg.2161

Table 1. Summary of the experimental data for SLV loci of different binary and ternary systems of CH_4, CO_2 and H_2S.

Mixture	Temperature range (K)	Pressure range (Bar)	Reference
CH_4-CO_2	194.5–215.3	9.17–48.54	Donnelly and Katz[24]
	143.15–203.15	19.74–47.23	Pikaar[25]
	166.33–199.6	19.47–49.61	Sterner[26]
	97.54–211.71	0.28–48.68	Davis et al.[27]
CH_4-H_2S	167.1–184.9	0.32–20.68	Kohn and Kurata[33]
CO_2-H_2S	177.9–215.6	0.35–5.02	Sobocinski and Kurata[37]
CH_4-CO_2-H_2S	199.44 –207.59	24.04–43.21	Langé[38]
	192–210	18.48–22.24	Théveneau *et al.*[39]

compositions were measured in the temperature ranges from 129.65 to 201.26 K and from 140.93 to 205.71 K, respectively. Figure 1(B) illustrates the composition of carbon dioxide in liquid and vapor phases. Experimental data for this binary system cover a wide range of temperature and pressure; and laboratory data available are close to each other as seen in Fig. 1. Table 1 summarizes the experimental data for the SLVE equilibrium of CH_4-CO_2 system.

From Fig. 1(A) it is clear that most of the experimental data follow the same SLVE locus curve trend, where the pressure will increase with temperature, until reaching a pressure peak value at a temperature of around 202 K, and then it will drop down reaching the triple point of CO_2. Within the SLVE locus curve envelop, two phases will be present: vapor and solid. While around this envelop liquid phase will be present as only liquid phase, liquid/solid phase, or liquid/vapor phase.

While laboratory data covering the vapor–liquid equilibrium of the binary system CH_4-H_2S are abundant,[30–32] experimental data covering the SLVE of this system are limited. The main study covering the thermodynamics of this system was conducted by Kohn and Kurata.[33] They developed an experimental setup for determining the solid phase behavior of the CH_4-H_2S system, six mixtures of methane and hydrogen sulfide were tested, the system temperature was varied between from −300 to 300°F (88.7–422 K), and pressures reaching up to 2000 psia (137.9 bar). For this binary system, there are two SLVE loci: the SL_1VE locus and the SL_2VE locus (where L_1 is the liquid phase that is rich with CH_4 and L_2 is the liquid phase that is rich with H_2S), where the solid phase consists of pure hydrogen sulfide. The SL_1VE and SL_2VE loci meet at the quadruple point (QP) at which four phases are

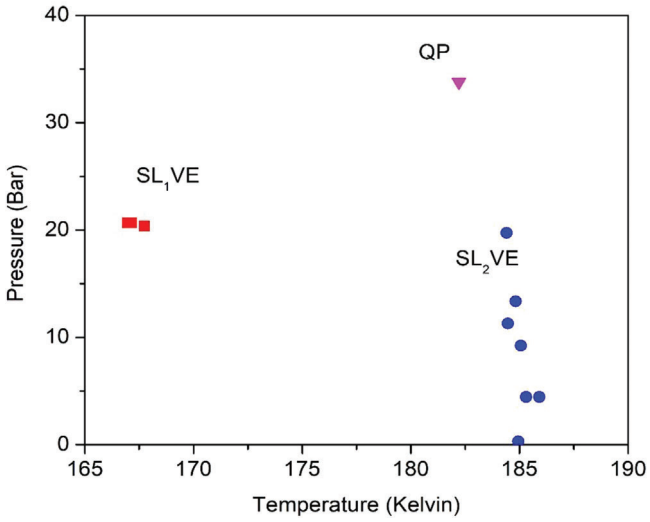

Figure 2. Measured pressure–temperature SLVE locus of the binary system CH_4-H_2S.[33]

present, that is, S, L_1, L_2, and VE. The results obtained for the SLVE locus of this binary system are shown in Fig. 2. Within the these point and below the QP point, two phases are only present: a pure solid H_2S phase and a vapor phase (which consists of both components). Table 1 lists the experimental data available for this binary system, it could be noticed that more works might be needed to confirm and expand the laboratory data available.

Similar to the CH_4-H_2S binary system, there are many experimental studies covering the VLE of the CO_2-H_2S system.[34–36] However, only the study by Sobocinski and Kurata[37] covered the SLVE of this binary system. They have conducted an experimental investigation that covered the region from the critical locus of the mixture to the SLVE region. Seven mixtures were tested individually to determine the phase diagrams

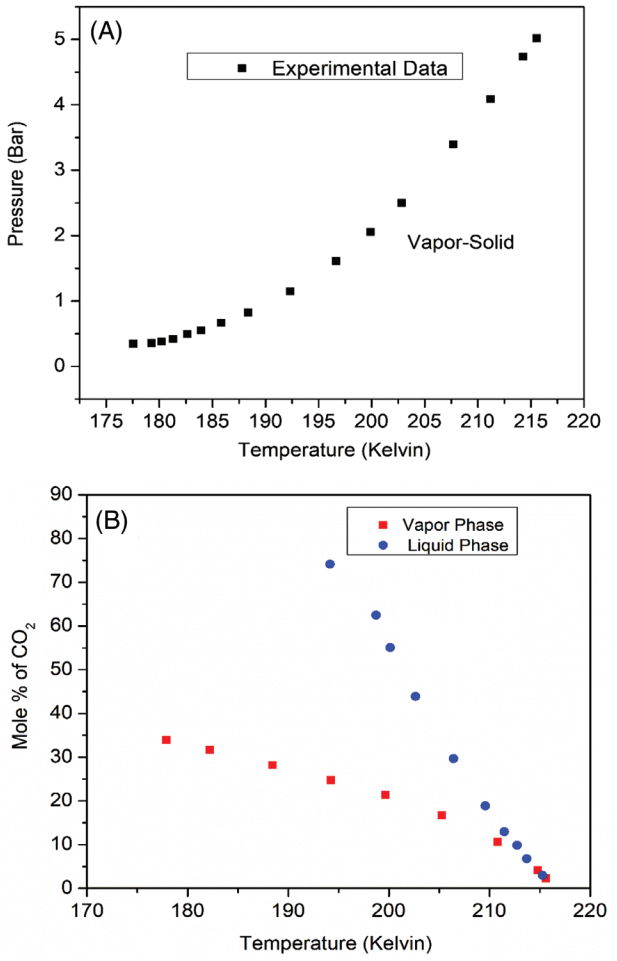

Figure 3. Experimental data (symbols) available for the binary system CO_2-H_2S in terms of (A) SLVE pressure-temperature locus and (B) corresponding CO_2 compositions in the liquid and vapor phases.[37]

and the compositions of each phase at the specified conditions. It was observed that SLVE locus is at temperatures lower than triple point of either pure CO_2 and H_2S, which was explained by the formation of a eutectic mixture (with a composition of 12.5 mole% CO_2 for all mixtures). Figure 3(A) illustrates the SLVE locus of the CO_2-H_2S binary system, which ends up near to the triple point of CO_2 (216.58 K, 5.185 bar[28]). Below this line, both vapor and solid phases are found. Above this line, liquid phase can be present with either solid or vapor phases. Figure 3(B) shows the composition of the vapor and liquid phases alongside the SLVE locus, where the solid phase consisted of pure CO_2.[37] The experimental data for the CO_2-H_2S system found in Fig. 3 and Table 1 is limited. Therefore, more research is recommended to be done to determine SLVE locus of this system experimentally.

Table 2. Compositions of the five mixtures tested for solidification point.[39].

Mixture	Z_{CH_4}	Z_{CO_2}	Z_{H_2S}	P (bar)	T_{exp} (K)
1	0.7993	0.2007	0	22.24	209.80
2	0.7603	0.1899	0.0498	21.86	202.33
3	0.7192	0.1806	0.1002	18.48	196.85
4	0.6802	0.1701	0.1497	19.74	194.32
5	0.6395	0.1604	0.2001	21.23	192.26

Experimental data, which covers the solid phase in the CH_4-CO_2-H_2S ternary system are rare and have limited temperature and pressure ranges. Langé *et al.*[38] designed an experimental procedure to obtain the *T-P-x-y* data for the region in which the SLVE locus exists for different compositions of this ternary system. However, their study covered only the region that contains solid CO_2 phase, and the temperature and pressure ranges were very limited (from 199.44 to 207.59 K and 14.599 to 43.212 bar, respectively). Théveneau *et al.*[39] utilized a visual synthetic laboratory technique to determine the freezing point of five different compositions of the ternary system CH_4-CO_2-H_2S. Table 2 lists the mole% of each component in these mixtures, where Z_i is the overall composition of component *i* in the mixture. However, this study also covered very limited ranges of temperature and pressure (192–210 K and 18.48–22.24 bar, respectively). Similar to the two binary systems CH_4-H_2S and CO_2-H_2S, the ternary system of the CH_4-CO_2-H_2S available in the literature are limited (Table 1), and more work is needed to expand our knowledge and develop more accurate phase envelopes for such system.

Modeling of SLVE systems

There are three major approaches to model the three-phase, SLVE of different systems. The first approach utilizes equations of state (EoS) for calculating the liquid and vapor phase fugacities, along with an independent model for the fugacity of the solid phase. The first approach could be further classified according to the model used to estimate the solid phase fugacity; such as the empirical correlation model,[40] thermodynamic integration model,[41] and Gibbs free energy EoS model.[42] The second approach depends on using an EoS for calculating the fugacities of the three phases the same time.[22] A completely different

approach was used by Ali *et al.*[43] to predict the SLVE locus curve, where they developed a predictive model that utilizes artificial neural networks (ANN), and the ANN predictions were compared to the experimental data. The following subsections highlight the use of these approaches for describing the SLVE locus and compositions of different binary and ternary systems considered in this review.

Modeling of SLVE for the binary system of CH_4-CO_2

Approach 1: Coupling EoS with specific models of solid phase fugacity

Nikolaidis *et al.*[40] have used an empirical correlation model to represent the equilibrium of the CH_4-CO_2 system. At equilibrium, the solid-phase fugacity of any compound equals the fugacity of that compound in the two coexisting fluid phases, that is:

$$\widehat{f}_i^S(T,P) = \widehat{f}_i^F\left(T,P,x^F\right) \quad (1)$$

Where the solid phase and fluid (vapor or liquid) phase fugacities of component i ($\hat{f}_i^S$ and $\hat{f}_i^F$, respectively) can be found from Eqns 2 and 3, respectively; and the solid phase consists of pure component i.

$$\widehat{f}_i^S(T,P) = \widehat{\varphi}_{0i}^{\mathrm{Sat}}\left(T,P_i^{\mathrm{Sat}}\right)P_{0i}^{\mathrm{Sat}}(T) \quad (2)$$

$$\times \exp\left[\frac{v_{0i}^s}{RT}\left(P - P_{0i}^{\mathrm{Sat}}(T)\right)\right] \quad (2)$$

$$\widehat{f}_i^F\left(T,P,x^F\right) = x_i^F\widehat{\varphi}_i^F\left(T,P,x^F\right)P \quad (3)$$

where $P_{0i}^{\mathrm{Sat}}(T)$ is the saturation/sublimation pressure of the solid forming component at the specified temperature T, $\widehat{\varphi}_{0i}^{\mathrm{Sat}}(T,P_i^{Sub})$ is the fugacity coefficient of the solid component at T and the saturation pressure P_{0i}^{Sat}, P is pressure, $\widehat{\varphi}_i^F(T,P,x^F)$ is the fugacity coefficient of the component i in the fluid mixture of molar composition x^F at T and P, and $v_{0i}^s$is the solid phase molar volume of the component i.

To utilize Eqns 1–3, Nikolaidis *et al.*[40] used three different equations of state (EoS) for determining the fugacities of vapor and liquid phases; namely, the Peng–Robinson (PR) EoS, Soave–Redlich–Kwong (SRK) EoS, and the perturbed-chain statistical associating fluid theory (PC-SAFT) EoS. Each of these equations included an interaction parameter between CO_2 and CH_4, k_{ij}, that was altered to optimize the model estimations of the experimental data. Overall, it was found that utilizing the PR EoS with $k_{ij} = 0.100$ resulted in the least error of model estimations compared to the experimental data,[24,27] with an average absolute deviation (AAD) (as defined in Eqn 4) of 2.19%. Figure 4(A) shows their estimated SLVE locus as generated using the PR EoS against experimental data.[24,27] To avoid crowding, only the data from Davis *et al.*[27] and Donnelley and Katz[24] were presented in Fig. 4 since they cover the widest ranges of temperatures and pressures.

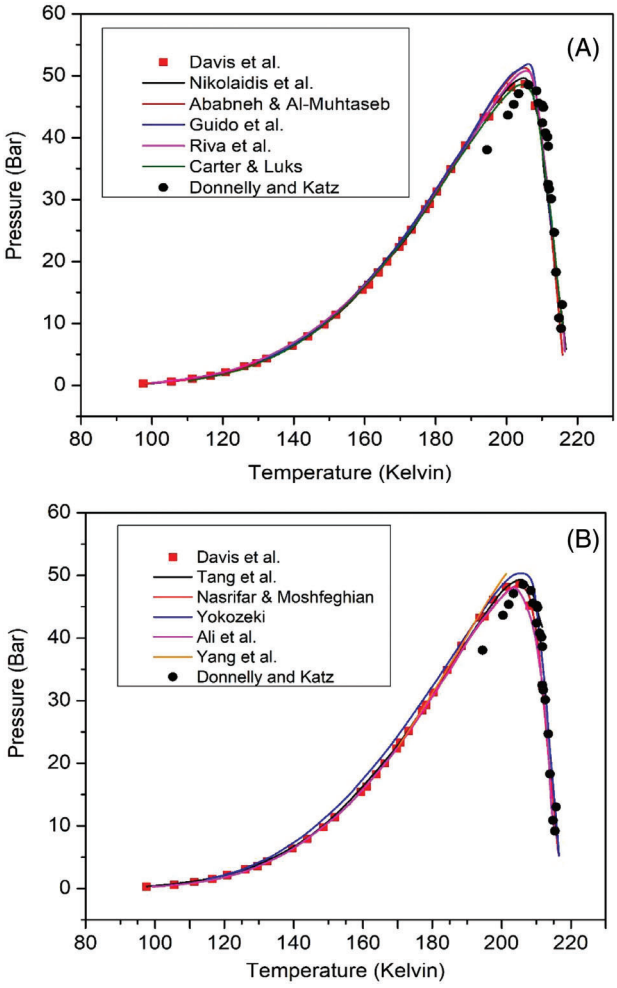

Figure 4. Comparison between models predictions (lines) with laboratory data (symbols)[24, 27] for the SLVE of the system CH_4-CO_2 system. Comparisons are divided between two subfigures to avoid overcrowding: (A)[27,40,44,48,2,49] (B) [50–52,43]

$$\%AAD = \frac{100}{N}\sum_{i=1}^{N}\left|\frac{P_i^{\mathrm{calculated}} - P_i^{\mathrm{experimental}}}{P_i^{\mathrm{experimental}}}\right| \quad (4)$$

where N is the number of experimental data points.

Ababneh and Al-Muhtaseb[44] utilized a similar technique to model the SLVE of various systems, including the binary system of CH_4-CO_2. They substituted Eqn 5[45] into Eqn 2 to find the fugacity of the solid phase (which consists of pure CO_2), whereas the vapor and liquid phase fugacities were calculated using the PR EoS with an optimized k_{ij} value of 0.12. The AAD in predicting the SLVE locus pressure at different pressures was 2.14%. Figure 4(A) shows a comparison of their estimated SLVE locus with experimental data.[24,27]

$$\ln\left(\frac{P^{Sub}_{CO_2}}{P_t}\right) = \frac{T_t}{T}\left[-14.740846\left(1-\frac{T}{T_t}\right)\right. \quad (5)$$

$$+2.4327015\left(1-\frac{T}{T_t}\right)^{1.9} \quad (5)$$

$$\left. + - 5.3061778\left(1-\frac{T}{T_t}\right)^{2.9}\right] \quad (5)$$

where T_t and P_t are the triple point temperature and pressure of CO_2, respectively; and $P^{Sub}_{CO_2}$ is the sublimation pressure of solid CO_2. Similar to the work of Ababneh and Al-Muhtaseb,[44] Yang *et al.*[46] studied the SLVE behavior of this system by combining the PR EoS with Eqn 6 to find the fugacities of fluid and solid phases, receptively. They found that the optimum value for the interaction parameter k_{ij} is 0.123, which is similar to the value found by Ababneh and Al-Muhtaseb. However, the study of Yang *et al.* covered a limited range of temperature (170–202 K) for the SLVE equilibrium. Their model predictions are compared to the experimental data[24,27] in Fig. 4(B).

$$ln\varphi^{s}_{\text{pure}} = ln\left(\varphi^{L}_{\text{pure}}\right) - \frac{\Delta H_f}{RT_m}\left[\frac{T_m}{T}-1\right] + \frac{\Delta c_p}{R}\left[\frac{T_m}{T}-1+\ln\left(\frac{T}{T_m}\right)\right] - \frac{\Delta v\left(p-p_m\right)}{RT} \quad (6)$$

where R is the universal gas constant, T is temperature, $\varphi^{L}_{\text{pure}}$ is the fugacity coefficient of the pure component in the liquid phase, and p_m is the reference pressure (triple point pressure for CO_2). For a pure component at p_m, T_m is the melting temperature, ΔH_f is the enthalpy of fusion, Δc_p is the change of the heat capacity upon the transition from the solid phase to liquid phase; and Δv is the change in molar volume upon transition from the solid phase to the liquid phase.

Riva *et al.*[2] proposed to calculate the solid phase fugacity of CO_2 by Eqns 7 and 8. This model is based on the numerical continuation method (NCM) of Rodriguez–Reartes *et al.*[47] The AAD of the corresponding predictions when compared to the experimental data was found to be 1.94%.[27] Fig. 4(A) compare the model predictions with experimental data.[24,27]

$$\widehat{f}^{S}_{i}(T, v_0) = \widehat{f}^{L}_{i}(T, 1, v_0)\exp(U) \quad (7)$$

$$U(T,P) = \frac{\Delta v^{S-L}}{RT}\left[-1.0819\times10^{-9}\left(1-\frac{T_t}{T}\right) + 3.5919\times10^{-6}\left(\frac{T_t}{T}-1+\ln\frac{T}{T_t}\right) + 4.2722\times10^{-6}\left(\frac{T}{2T_t}-1+\frac{T_t}{2T}\right) + \frac{T_t}{T}(\mathrm{P}-P_t)\right] \quad (8)$$

where v_0 (m^3/mol) is the molar volume of CO_2 in the hypothetical subcooled liquid state at T (K) and P (MPa). Furthermore, T_t and P_t are the triple-point temperature (in kelvin) and pressure (in MPa); and Δv^{S-L} is the solid−liquid molar volume difference of CO_2 (in m^3/mol).

Carter and Luks used a mathematical artifice to predict the solid CO_2 fugacity, and it was combined with the SRK EoS to find the SLVE locus.[49] The mathematical artifice was developed by Prausnitz *et al.*[53] as shown in Eqn 9. The interaction parameter k_{ij} in the EoS was varied between 0.10 and 0.13, and the results were compared to experimental data[27,24] as shown in Fig. 4(A).

$$\ln\frac{f}{f_s} = \frac{(H-H_s)-\left(H-H_{s,t}\right)}{RT} - \frac{(S-S_t)-(S-S_t)}{R} \quad (9)$$

where the subscripts s and t indicate the solid phase and triple point, respectively. S is the entropy, and f is the fugacity of liquid or gas phase of the pure component.

Similarly, Guido *et al.*[48] proposed a method based on each of the PR and SRK equations of state to predict the SLVE. Equation 10 was used to calculate the fugacity of the solid CO_2 phase starting from the liquid

phase fugacity. Their SLVE locus predictions (using the SRK EoS) are shown in Fig. 4(A).

$$\ln \frac{f^s(T,P)}{f^L(T,P)} = \frac{\Delta h_m}{RT_m}\left(1-\frac{T_m}{T}\right) - \frac{\Delta C_P\,(T_m - T)}{RT} - \frac{\Delta C_P}{R}\ln\frac{T_m}{T} \tag{10}$$

where Δh_m is the enthalpy change of melting, ΔC_P is the change of heat capacity between liquid and solid phases. Superscripts s and L indicate the solid and the liquid phases, respectively; and subscript m denotes the melting point.

Tang *et al.*[50] estimated the solid CO_2 fugacity by first calculating the minimum Gibbs free energy (g) by an algorithm that involves a stability variable of vapor or liquid phases, which was developed using composition-independent correlations of solid−vapor and solid−liquid equilibria as the initial estimation for the phase fraction, and then plugging its value in Eqn 11;[50] where the superscripts s, and 0 represent the solid and ideal gas phases, respectively. The resulted SLVE locus curve compared to the experimental data,[24,27] with an AAD of 1.98%, is also shown in Fig. 4(B).

$$f^s = f^0 \exp\left[\frac{g^s - g^0}{RT}\right] \tag{11}$$

Nasrifar and Moshfeghian developed a relation for the solid fugacity of CO_2 based on the triple point of carbon dioxide as seen in Eqn 12.[51] This equation, coupled with the Nasrifar-Bolland (NB) EoS, was used to predict the SVE and SLVE loci for CH_4-CO_2 system. Figure 4(B) shows the results obtained by the model compared to the data by Davis *et al.*[27] and Donnelley and Katz.[24]

$$f^s(T,P) = f^s(T_t,P_t)\exp\left[\frac{v^s(P-P_t)}{RT} - \frac{\Delta H_{sub}}{RT}\left(1-\frac{T}{T_t}\right)\right] \tag{12}$$

where $v^s$is the molar volume of the solid phase and $\Delta H_{sub}$is the enthalpy change at sublimation. Ababneh and Al-Muhtaseb[44] have been successful in predicting the distrbution of CH_4 and CO_2 between the three phase, where they assumed the solid phase to consist of pure CO_2. Figure 5 shows their results comapred to the experimental data.[24,27]

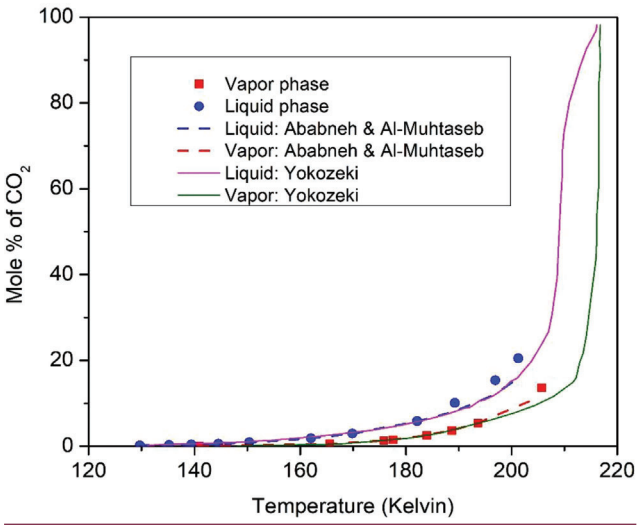

Figure 5. Model predictions (lines) compared to experimental data (symbols)[27] for the distribution of CH_4 CO_2 in the liquid and vapor phases.[44,52]

Approach 2: Using EoS for vapor, liquid, and solid phases

Yokozeki proposed an analytical EoS that is capable of representing the three phases: vapor, liquid, and solid.[52] Eq. 13 shows the pressure explicit form of this equation.

$$P(T,v) = \frac{RT}{v-b}\left(\frac{v-d}{v-c}\right)^k - \frac{a}{v^2+qbv+rb^2} \tag{13}$$

where c, b, a are the liquid covolume, the solid covolume, and a parameter of attractive forces between molecules, respectively; while d, k, q, and r are fitting parameters. While the results of Yokozeki were in good agreement with the experimental pressure-temperature locus data[27] as seen in Fig. 4(B), the issue with this model is that its predictions assume the presence of methane (up to 3%) in the solid phase, which is unrealistic.

Furthermore, Yokozeki's model[52] has successfully described the experimental composition data of Davis *et al.*[27] as seen in Fig. 5. However, there is an apparent deviation between the model predictions and experimental data at high temperatures, which could be explained by the fact the model assumes a presence of methane in the solid phase, even at higher temperatures; thus altering the model calculations for the other two phases. On the other hand, Ababneh and Al-Muhtaseb's model resulted in better predictions for the experimental data in the vapor phase as shown in

Table 3. Comparison between the model AAD values for the different studies predicting SLV locus of the CH_4-CO_2 system.

Model	AAD%	Experimental data compared
Nikolaidis *et al.*[40]	2.19%	Davis *et al.*[27] Donnelly and Katz[24]
Ababneh & Al-Muhtaseb[44]	2.14%	Davis *et al.*[27]
Riva *et al.*[2]	1.94%	Davis *et al.*[27]
Tang[50]	1.98%	Davis *et al.*[27]
Yokozeki[52]	2.05%	Davis *et al.*[27,*]
Ali et al.[43]	0.1447%	Davis *et al.*[27]

*As reported in Riva *et al.*[2]

Fig. 5, which could be attributed to their assumption that the solid phase consists of pure CO_2, in agreement with experimental observations. On the other hand, both model showed good agreemt with experimental data in the liquid phase.

Approach 3: Using artificial neural networks (ANN)

Ali *et al.*[43] utilized a different approach to predict the SLVE locus for the CH_4-CO_2 binary system. An artificial neural network (ANN) was developed by the following procedure: Data collection and preprocessing, creating, and optimizing the ANN design, training the ANN using the previously collected data sets and finally comparing predictions to the experimental data for validation. When compared to Davis *et al.* data,[27] the ANN predictions resulted in an AAD% of 0.1447% as seen in Fig. 4(B). While the ANN had excellent results, it is seen as an unnecessary tool in the presence of simpler thermodynamic models, which are able to produce similar results. The complication of ANN could be a more useful technique in case of complicated systems, which cannot be described easily by simple mathematical models. However, in this case it does not appear to make a case for itself. Table 3 compares the model AAD values to the experimental data.

Modeling the binary system of CH_4-H_2S

Only a limited number of studies attempted to model the SLVE of the CH_4-H_2S binary system using the first two approaches. These studies are highlighted below according to the corresponding approach.

Approach 1: Coupling EoS with specific models of solid phase fugacity

As discussed in the previous section, Ababneh and Al-Muhtaseb[44] have used an empirical correlation model to represent the CH_4-H_2S SLVE locus, where they substituted Eqn 14[54] in Eqn 2 to calculate the fugacity of the solid phase of H_2S.

$$\log_{10}\left(P_{H_2S}^{Sub}\right) = 7.22418 - \frac{118.0}{T} - 0.196426T + 0.0006636T^2 \quad (14)$$

where $P_{H_2S}^{Sub}$ is the sublimation pressure of H_2S (in cm Hg), and T is the temperature (in K).

Approach 2: Using EoS for vapor, liquid, and solid phases

Langè *et al.*[38] have studied the phase equilibrium behavior of the system CH_4-H_2S, at temperatures ranging from 70 K up to the critical temperature of H_2S (373.1 K) and pressures up to 25 bar.[31] Phase diagrams for this binary system at the SLVE locus have been found using the solid–liquid–vapor equation of state proposed by Yokozeki.[52]

Figure 6 shows the results of these two studies compared to the experimental data.[33] From Fig. 6, it is clear that the correlations of Lange *et al.* are more accurate than those by Ababneh and Al-Muhtaseb, which could be explained by the fact that Yokozeki's EoS does not consider the solid phase to be pure H_2S, which gives the equation more flexibility in predicting the locus curve, thus resulting in better representative correlations.

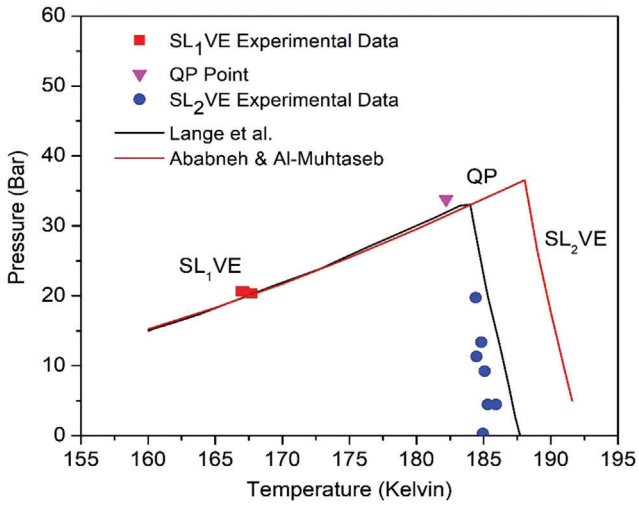

Figure 6. Comparison between model predictions (lines)[31,44] and laboratory data (symbols)[33] for the SLVE locus of the methane-hydrogen sulfide system.

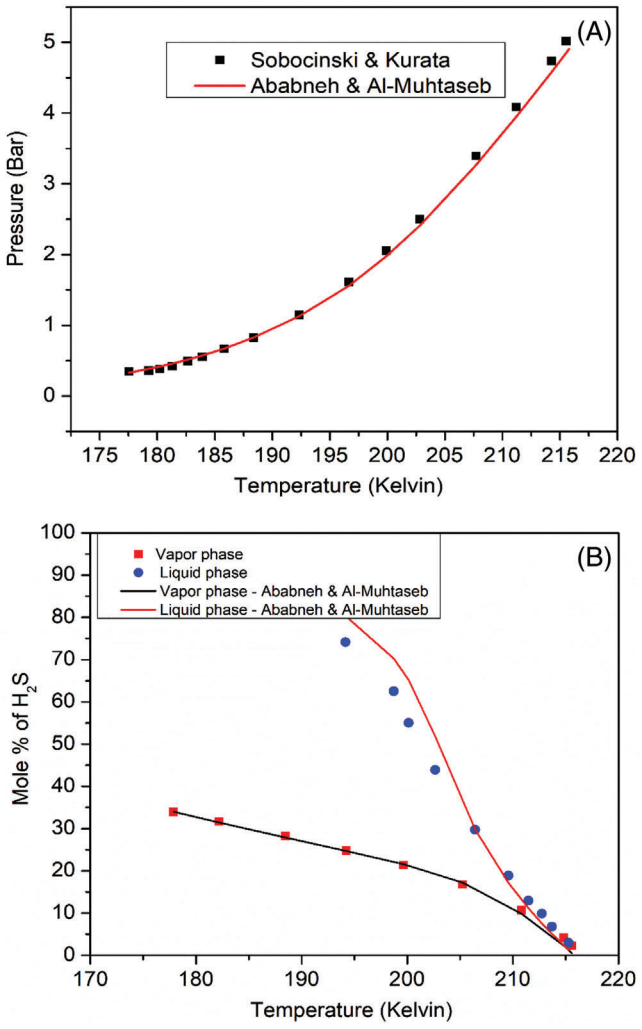

Figure 7. Model predictions (lines) compared to the experimental data (symbols) for the binary system CO_2-H_2S in terms of (A) the SLVE locus[37,44] and (B) the composition of H_2S in the liquid and vapor phases.[37,44]

Modeling the binary system of CO_2-H_2S

Little work has been done on modeling the SLVE locus of CO_2-H_2S system. The main modeling efforts were focused on the VLE of this binary system.[55–57] The only study that addressed the SLVE of this system was by Ababneh and Al-Muhtaseb,[44] where they successfully predicted the SLVE locus curve and the distrbution of H_2S and CO_2 between the three phase. They utlized an empirical correlation model in their study, which covered the temperature range slightley above the solidfication point of H_2S within the mixture (from 177.54 K up to 215.8 K). Thus, in the studied range of temperature, the solid phase was assumed to consist of pure CO_2, and Eqn 2 was used to find the fugacity of the solid CO_2 phase. Furthermore, the vapor and liquid phase fugacities were calculated using the PR EoS.[58] The interaction parameter between the two components was optimized to experimental data[37] to a value of 0.11, which resulted in total error of 14.1%. The total error was calcuated based on the errors in pressure, liquid phase composition, and vapor phase composition comapred to the experimental data by Sobocinski and Kurata.[37] Their results agreed very well with the experimental data as shown in Figs 7(A and B).

Modeling the ternary system of CH_4-CO_2-H_2S

Theveneau *et al.*[39] have utilized four equations of state, which are based on the group contribution method; the PPR78 (predictive, 1978 Peng Robinson) EoS,[59] the PSRK (Soave–Redlich–Kwong) EoS,[60] a semi-empirical EoS, and the PR-HV (Peng Robinson–Huron–Vidal mixing rule) EoS with the NRTL activity model;[61] to predict the CO_2 freezing temperatures.[39] Ababneh and Al-Muhtaseb[44] developed an empirical model based on Peng Robinson equation of state (PR EoS)[58] with fugacity expressions for the solid, and fluid phases (Eqns 2 and 3, respectively). Their model predicts and describes the SLVE for CH_4-CO_2-H_2S ternary system over much expanded pressure and temperature ranges (5–30 bar and 130–200 K, respectively). Table 4 compares the results of the above mentioned studies,[39,44] to the experimental data obtained by

Table 4. Comparison between the different studies for the ternary system of CH_4-CO_2-H_2S.

	Theveneau *et al.*[39]		Ababneh and Al-Muhtaseb[44]		Theveneau *et al.*[39]							
					PPR78[59]		PSRK UNIFAC[60]		PR-HV /NRTL-V[61]	GERG 2008 (REFPROP)[62]		GERG 2008 (REFPROP)with Jager and Span model[42]
Mixture	P (MPa)	T_{exp} (kelvin)	T_{pred} (kelvin)		T_{pred} (kelvin)		T_{pred} (kelvin)		T_{pred} (kelvin)	T_{pred} (kelvin)		T_{pred} (kelvin)
1	2.224	209.80	213.03		209.67		210.31		210.45	210.54		210.26
2	2.186	202.33	203.74		208.5		209.18		203.15	209.28		209.03
3	1.848	196.85	200.05		173.06		185.91		198.85	193.25		192.75
4	1.974	194.32	197.62		167.93		181.54		195.15	189.91		189.26
5	2.123	192.26	195.43		163.18		177.99		191.45	186.98		186.27
MAD (K)			2.86		17.11		9.07		1.02	4.2		4.46
MRD (%)			1.44%		8.78%		4.63%		0.52%	2.12%		2.27%

Table 5. Different cases of feed compositions tested by Ababneh and Al-Muhtaseb.[44].

Feed Mixture	CH_4 mole%	CO_2 mole%	H_2S mole%
Case "A"	80	15	5
Case "B"	80	10	10
Case "C"	50	30	20

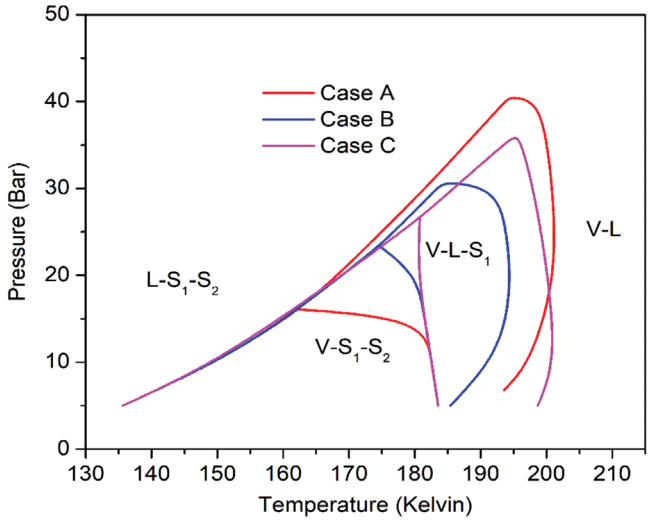

Figure 8. Pressure-temperature phase diagrams for the three cases studied by Ababneh & Al-Muhtaseb.[44]

Theveneau *et al.*;[39] where MAD and MRD are defined in Eqns 15 and 16, respectively. It could be noticed from Table 4 that PR-HV/NRTL and Ababneh and Al-Muhtaseb models have the best predictions of the experimental data.

$$\mathrm{MAD} = \frac{1}{N}\sum \left|U_{\mathrm{cal}} - U_{\mathrm{exp}}\right| \tag{15}$$

$$\mathrm{MRD} = \frac{100}{N}\sum \left|\frac{U_{\mathrm{cal}} - U_{\mathrm{exp}}}{U_{\mathrm{exp}}}\right| \tag{16}$$

where U is the property; and subscripts cal and exp denote, respectively, the calculated and experimental values.

Furthermore, Ababneh and Al-Muhtaseb[44] simulated an equilibrium stage separation unit, which was based on their designed model. This unit was used to simulate the separation of the CH_4-CO_2-H_2S ternary system with three cases of different feed compositions (see Table 5). The unit's performance was evaluated for each case at different pressures and temperatures. The predicted phase diagrams for the three cases are shown in Fig. 8; where S_1 and S_2 represent the solid phases of

Greenhouse. Gas. Sci. Technol. **12**:566–579 (2022); DOI: 10.1002/ghg.2161

CO_2 and H_2S, respectively. Figure 8 shows that decreasing the H_2S/CO_2 ratio in the feed results in higher melting temperatures. On the other hand, the H_2S/CH_4 ratio affects the V-S_1-S_2/ V-L-S_1 equilibrium line, where a higher H_2S/CH_4 ratio in the feed makes the V-S_1-S_2 region cover wider ranges of temperature and pressures. This could be attributed the solidification temperature of H_2S, which is higher than that of CH_4. Therefore, increasing H_2S in the feed moves the V-S_1-S_2/ V-L-S_1 equilibrium line to higher temperature.

Conclusions

This article reviewed the SLVE for the acid gases (CO_2 and H_2S) in natural/biogas; which consists mainly of CH_4. It covered the binary systems of CH_4-CO_2, CH_4-H_2S and H_2S-CO_2; as well as the ternary system of CH_4-H_2S-CO_2. It includes the experimental data available in the literature as well as the models used to predict these data. Moreover, this review compared the predictions of the models and their accuracies.

Despite of the importance of studying the phase behavior of acid gases in the natural/biogas, it could be concluded that the available scientific literature is very rare, especially for the binary systems CH_4-H_2S and H_2S-CO_2 and the ternary system of CH_4-H_2S-CO_2, which stresses the importance of modeling efforts for such systems. The experimental data available can sometimes be outdated or not covering wide ranges of pressures and temperatures. The models used to predict the SLVE phase behaviors proved successful in most cases, this suggests expanding these models to cover the SLVE of other systems relevant to different industries such as air separation and noble gases production. However, models based on some equations of state, which are able to calculate the fugacity for the three phases (such as Yokozeki's equation of state[52]), are assuming the presence of methane in the solid phase, which is inconsistent with data found in experimental studies. Therefore, it is advisable to alter these models to better represent such cases. The artificial neural network technique to predict the SLVE proved accurate, but it might be more complicated than the more traditional models and techniques that are showing acceptably good results. Furthermore, it is recommended to conduct further experimental and theoretical studies using state-of-the-art and modern equipment or techniques to specify and determine accurately the SLVE phase diagrams for these systems.

Acknowledgments

Open Access funding provided by the Qatar National Library.

Conflict of interest

The authors declare no conflict of interest.

References

1. British Petroleum, "Energy Outlook 2020," 2020. [Online]. Available:https://www.bp.com/content/dam/bp/business-sites/en/global/corporate/pdfs/energy-economics/energy-outlook/bp-energy-outlook-2020.pdf
2. Riva M, Campestrini M, Toubassy J, Clodic D, Stringari P. Solid-liquid-vapor equilibrium models for cryogenic biogas upgrading. Ind Eng Chem Res. 2014;53(44):17506–14. https://doi.org/10.1021/ie502957x
3. Esteves IAAC, Lopes MSS, Nunes PMC, Mota JPB. Adsorption of natural gas and biogas components on activated carbon. Sep Purif Technol. 2008;62(2):281–96. https://doi.org/10.1016/j.seppur.2008.01.027
4. Mondal MK, Balsora HK, Varshney P. Progress and trends in CO2 capture/separation technologies: A review. Energy. 2012;46(1):431–41. https://doi.org/10.1016/j.energy.2012.08.006
5. International Energy Agency. CO_2 emissions from fuel combustion 2017; 2017.
6. IPCC. Global warming of 1.5°C An IPCC Special Report on the impacts of global warming of 1.5°C above pre-industrial levels and related global greenhouse gas emission pathways, in the context of strengthening the global response to the threat of climate change; 2018.
7. Fowler CM. 2.11 - Cracking stimulated by hydrogen. In: Cottis B, Graham M, Lindsay R, Lyon S, Richardson T, Scantlebury D, Stott HBTSC, editors. Shreir's corrosion. Oxford: Elsevier; 2010. p. 923–927.
8. Ropp RC. Chapter 3 - Group 16 (O, S, Se, Te) alkaline earth compounds. In: Ropp RC, editor. Encyclopedia of the alkaline earth compounds. Amsterdam: Elsevier; 2013, p. 105–197.
9. Pouliquen F, Blanc C, Arretz E, Labat I, Tournier-Lasserve J, Ladousse A, *et al*. Hydrogen sulfide. In: Ullmann's encyclopedia of industrial chemistry. Wiley; 2000, https://doi.org/10.1002/14356007.a13_467
10. Wang M, Lawal A, Stephenson P, Sidders J, Ramshaw C. Post-combustion CO_2 capture with chemical absorption: A state-of-the-art review. Chem Eng Res Des. 2011;89(9):1609–24. https://doi.org/10.1016/j.cherd.2010.11.005
11. Maqsood K, Mullick A, Ali A, Kargupta K, Ganguly S. Cryogenic carbon dioxide separation from natural gas: A review based on conventional and novel emerging technologies. Rev Chem Eng. 2014;30(5):453–77. https://doi.org/10.1515/revce-2014-0009
12. Ali A, Maqsood K, Redza A, Hii K, Shariff ABM, Ganguly S. Performance enhancement using multiple cryogenic desublimation based pipeline network during dehydration and carbon capture from natural gas. Chem Eng Res Des. 2016;109:519–31. https://doi.org/10.1016/j.cherd.2016.01.020

13. Valencia JA, Denton RD, Northrop PS, Mart CJ, Smith RK. Controlled freeze zone technology for the commercialization of Australian high CO2 natural gas. Soc. Pet. Eng. - SPE Asia Pacific Oil Gas Conf. Exhib. APOGCE 2014 - Chang. Game Oppor. Challenges Solut. 2014;2:951–61. https://doi.org/10.2118/171508-ms
14. Font-Palma C, Cann D, Udemu C. Review of cryogenic carbon capture innovations and their potential applications. C. 2021;7(3):58. https://doi.org/10.3390/c7030058
15. Ali A, Maqsood K, Syahera N, Shariff ABM, Ganguly S. Energy minimization in cryogenic packed beds during purification of natural gas with high CO_2 content. Chem Eng Technol. 2014;37(10):1675–85. https://doi.org/10.1002/ceat.201400215
16. Tuinier MJ, van Sint Annaland M, Kramer GJ, Kuipers JAM. Cryogenic CO_2 capture using dynamically operated packed beds. Chem Eng Sci. 2010;65(1):114–9. https://doi.org/10.1016/j.ces.2009.01.055
17. Willson P, Lychnos G, Clements L, Michailos S, Font-Palma C, Diego ME, et al. Evaluation of the performance and economic viability of a novel low temperature carbon capture process. Int J Greenh Gas Control. 2019;86:1–9. https://doi.org/10.1016/j.ijggc.2019.04.001
18. Song C-F, Kitamura Y, Li S-H, Ogasawara K. Design of a cryogenic CO_2 capture system based on Stirling coolers. Int J Greenh Gas Control. 2012;7:107–14. https://doi.org/10.1016/j.ijggc.2012.01.004
19. Jensen MJ, Russell CS, Bergeson D, Hoeger CD, Frankman DJ, Bence CS, *et al*. Prediction and validation of external cooling loop cryogenic carbon capture (CCC-ECL) for full-scale coal-fired power plant retrofit. Int J Greenh Gas Control. 2015;42:200–12. https://doi.org/10.1016/j.ijggc.2015.04.009
20. Kelley BT, Valencia JA, Northrop PS, Mart CJ. Controlled Freeze Zone™ for developing sour gas reserves. Energy Procedia. 2011;4:824–9. https://doi.org/10.1016/j.egypro.2011.01.125
21. Hart A, Gnanendran N. Cryogenic CO_2 capture in natural gas. Energy Procedia. 2009;1(1):697–706. https://doi.org/10.1016/j.egypro.2009.01.092
22. Tan Y, Nookuea W, Li H, Thorin E, Yan J. Cryogenic technology for biogas upgrading combined with carbon capture-a review of systems and property impacts. Energy Procedia. 2017;142:3741–6. https://doi.org/10.1016/j.egypro.2017.12.270
23. Babar M, Bustam MA, Ali A, Maulud AS, Shafiq U, Mukhtar A, *et al*. Thermodynamic data for cryogenic carbon dioxide capture from natural gas: a review. Cryogenics (Guildf). 2019;102(June):85–104. https://doi.org/10.1016/j.cryogenics.2019.07.004
24. Donnelly HG, Katz DL. Phase equilibria in the carbon dioxide–methane system. Ind Eng Chem. 1954;46(3):511–7. https://doi.org/10.1021/ie50531a036
25. Pikaar MJ. A study OP phase equilibria in hydrocarbon-CO_2 systems. University of London; 1959.
26. Sterner CJ. Phase Equilibria in the CO2-Methane Systems. In: Timmerhaus, KD (eds), Advances in Cryogenic Engineering. Advances in Cryogenic Engineering, vol 6. Springer, Boston, MA. 1961:467–474. https://doi.org/10.1007/978-1-4757-0534-8_49
27. Davis JA, Rodewald N, Kurata F. Solid-liquid-vapor phase behavior of the methane-carbon dioxide system. AIChE J. 1962;8(4):537–9. https://doi.org/10.1002/aic.690080423
28. Schneider GM. Carbon Dioxide - International Thermodynamic Tables of the Fluid State, Bd. 3. Von S. Angus, B. Armstrong und K. M. de Rerrck. Pergamon Press Ltd., Oxford-New York 1976. 1. Aufl., XXVII, 385 S., zahlr. Abb. u. Tab., geb., DM 172,50. Chemie Ingenieur Technik. 1977;49(7):594. https://doi.org/10.1002/cite.330490727
29. Angus S, Armstrong B, Reuck K M De. Methane: International Thermodynamic Tables of the Fluid State-5. Nuclear Techno. 1981;54(1):126. https://doi.org/10.13182/nt81-a32767
30. Yarym-Agaev NL, Afanasenko LD, Matvienko VG, Ryabkin YY, Tolmacheva GB. Gas-liquid equilibrium in the system methane - hydrogen sulphide at a temperature below 273K. Ukr Khimicheskii Zhurnal. 1991;57:701–4.
31. Langé S, Campestrini M, Stringari P, Langé S, Campestrini M, Stringari P. Phase behavior of system methane + hydrogen sulfide. AIChE J. 2017;62(11):4090–108.
32. Coquelet C, Valtz A, Stringari P, Popovic M, Richon D, Mougin P. Phase equilibrium data for the hydrogen sulphide+methane system at temperatures from 186 to 313K and pressures up to about 14MPa. Fluid Phase Equilib. 2014;383:94–99. https://doi.org/10.1016/j.fluid.2014.09.025
33. Kohn JP, Kurata F. Heterogeneous phase equilibria of the methane—hydrogen sulfide system. AIChE J. 1958;4(2):211–7. https://doi.org/10.1002/aic.690040217
34. Robinson DB, Lorenzo AP, Macrygeorgos CA. The carbon dioxide-hydrogen sulphide-methane system: Part II. Phase behavior at 40°f. and 160°f. Can J Chem Eng. 1959;37(6):212–7. https://doi.org/10.1002/cjce.5450370603
35. Chapoy A, Coquelet C, Liu H, Valtz A, Tohidi B. Vapour-liquid equilibrium data for the hydrogen sulphide (H_2S)+carbon dioxide (CO_2) system at temperatures from 258 to 313K. Fluid Phase Equilib. 2013;356:223–8. https://doi.org/10.1016/j.fluid.2013.07.050
36. Li H. Thermodynamic properties of CO_2 mixtures and their applications in advanced power cycles with CO_2 capture processes. Stockholm, Sweden: Royal Insititute of Techonology; 2008.
37. Sobocinski DP, Kurata F. Heterogeneous phase equilibria of the hydrogen sulfide–carbon dioxide system. AIChE J. 1959;5(4):545–51. https://doi.org/10.1002/aic.690050425
38. Langé S, Pellegrini LA, Stringari P, Coquelet C. Experimental de-termination of the solid-liquid-vapor locus for the ch 4 -co 2 -h 2 s system and application to the design of a new low-temperature distillation process for the purification of natural gas. in 94th GPA Convention, 2016.
39. Théveneau P, Fauve R, Coquelet C, Mougin P. Measurement and modelling of solid apparition temperature for the CO_2–H_2S–CH_4 ternary system. Fluid Phase Equilib. 2020;509:112465. https://doi.org/10.1016/j.fluid.2020.112465
40. Nikolaidis IK, Boulougouris GC, Peristeras LD, Economou IG. Equation-of-state modeling of solid-liquid-gas equilibrium of CO_2 binary mixtures. Ind Eng Chem Res. 2016;55(21):6213–26. https://doi.org/10.1021/acs.iecr.6b00669
41. Seiler M, Groß J, Bungert B, Sadowski G, Arlt W. Modeling of solid/fluid phase equilibria in multicomponent systems at high pressure. Chem Eng Technol. 2001;24(6):607–12. https://doi.org/10.1002/1521-4125(200106)24:6<607::AID-CEAT607>3.0.CO;2-T
42. Jäger A, Span R. Equation of state for solid carbon dioxide based on the Gibbs free energy. J Chem Eng Data. 2012;57(2):590–7. https://doi.org/10.1021/je2011677

43. Ali A, Abdulrahman A, Garg S, Maqsood K, Murshid G. Application of artificial neural networks (ANN) for vapor-liquid-solid equilibrium prediction for CH_4-CO_2 binary mixture. Greenh Gases Sci Technol. 2019;9(1):67–78. https://doi.org/10.1002/ghg.1833
44. Ababneh H, Al-Muhtaseb S. An empirical correlation-based model to predict solid-fluid phase equilibria and phase separation of the ternary system CH_4-CO_2-H_2S. J Nat Gas Sci Eng. 2021;94:104120. https://doi.org/10.1016/j.jngse.2021.104120
45. Span R, Wagner W. A new equation of state for carbon dioxide covering the fluid region from the triple-point temperature to 1100 K at pressures up to 800 MPa. J Phys Chem Ref Data. 1996;25(6):1509–96. https://doi.org/10.1063/1.555991
46. Yang X, Rowland D, Sampson CC, Falloon PE, May EF. Evaluating cubic equations of state for predictions of solid-fluid equilibrium in liquefied natural gas production. Fuel. 2022;314:123033. https://doi.org/10.1016/j.fuel.2021.123033
47. Rodriguez-Reartes SB, Cismondi M, Zabaloy MS. Computation of solid-fluid-fluid equilibria for binary asymmetric mixtures in wide ranges of conditions. J Supercrit Fluids. 2011;57(1):9–24. https://doi.org/10.1016/j.supflu.2011.02.004
48. De Guido G, Langè S, Moioli S, Pellegrini LA. Thermodynamic method for the prediction of solid CO_2 formation from multicomponent mixtures. Process Saf Environ Prot. 2014;92(1):70–79. https://doi.org/10.1016/j.psep.2013.08.001
49. Carter K, Luks KD. Extending a classical EOS correlation to represent solid-fluid phase equilibria. Fluid Phase Equilib. 2006;243(1–2):151–5. https://doi.org/10.1016/j.fluid.2006.02.021
50. Tang L, Li C, Lim S. Solid-liquid-vapor equilibrium model applied for a CH_4-CO_2 binary mixture. Ind Eng Chem Res. 2019;58(39):18355–66. https://doi.org/10.1021/acs.iecr.9b02389
51. Nasrifar K, Moshfeghian M. Prediction of carbon dioxide frost point for natural gas and LNG model systems. J Nat Gas Sci Eng. 2020;76(December 2019):103206. https://doi.org/10.1016/j.jngse.2020.103206.
52. Yokozeki A. Analytical equation of state for solid-liquid-vapor phases. Int J Thermophys. 2003;24(3):589–620. https://doi.org/10.1023/A:1024015729095.
53. Prausnitz JM, Lichtenthaler RN, de Azevedo EG. Solubilities of solids in liquids. In Prausnitz JM, Lichtenthaler RN, Gomes de Azevedo E, editors. Molecular thermodynamics of fluid-phase equilibria. 3rd ed. Pearson Education; 1998, p. 864.
54. Clark AM, Cockett AH, Eisner HS. The vapour pressure of hydrogen sulphide. Proc R Soc London Ser A Math Phys Sci. 1951;209(1098):408–15. https://doi.org/10.1098/rspa.1951.0214
55. Huron M-J, Dufour G-N, Vidal J. Vapour-liquid equilibrium and critical locus curve calculations with the soave equation for hydrocarbon systems with carbon dioxide and hydrogen sulphide. Fluid Phase Equilib. 1977;1(4):247–65. https://doi.org/10.1016/0378-3812(77)80008-3
56. Tsivintzelis I, Kontogeorgis GM, Michelsen ML, Stenby EH. Modeling phase equilibria for acid gas mixtures using the CPA equation of state. I. Mixtures with H2S. AIChE J. 2010;56(11):2965–82. https://doi.org/10.1002/aic.12207
57. Tang X, Gross J. Modeling the phase equilibria of hydrogen sulfide and carbon dioxide in mixture with hydrocarbons and water using the PCP-SAFT equation of state. Fluid Phase Equilib. 2010;293(1):11–21. https://doi.org/10.1016/j.fluid.2010.02.004
58. Peng D-Y, Robinson DB. A new two-constant equation of state. Ind Eng Chem Fundam. 1976;15(1):59–64. https://doi.org/10.1021/i160057a011
59. Jaubert J-N, Privat R, Mutelet F. Predicting the phase equilibria of synthetic petroleum fluids with the PPR78 approach. AIChE J. 2010;56(12):3225–35. https://doi.org/10.1002/aic.12232
60. Holderbaum T, Gmehling J. PSRK: a group contribution equation of state based on UNIFAC. Fluid Phase Equilib. 1991;70(2):251–65. https://doi.org/10.1016/0378-3812(91)85038-V
61. Huron M-J, Vidal J. New mixing rules in simple equations of state for representing vapour-liquid equilibria of strongly non-ideal mixtures. Fluid Phase Equilib. 1979;3(4):255–71.
62. Kunz O, Wagner W. The GERG-2008 wide-range equation of state for natural gases and other mixtures: an expansion of GERG-2004. J Chem Eng Data. 2012;57(11):3032–91. https://doi.org/10.1021/je300655b

Hani Z. Ababneh

Hani Z. Ababneh is PhD candidate in chemical engineering at Qatar University. He earned his MSc in sustainable energy from Hamad Bin Khalifah University in 2018. He earned his BSc degrees in Chemical Engineering from the Jordan University of Science and Technology. His main research areas cover process modeling and optimization, CO_2 capturing, and fuel characterization.

Shaheen A. Al-Muhtaseb

Shaheen A. Al-Muhtaseb is a Professor of Chemical Engineering at Qatar University. He earned his PhD degree in Chemical Engineering from the University of South Carolina in 2001. He also earned his MSc and BSc degrees in Chemical Engineering from the Jordan University of Science and Technology. His main research interests are the various fields of Advanced Materials, with special attention to adsorption equilibria, membranes for gas separation, and energy storage materials.